THE ASTROPHYSICAL JOURNAL, 628:L123–L126, 2005 August 1

EARLY-TIME *SPITZER* OBSERVATIONS OF THE TYPE II PLATEAU SUPERNOVA SN 2004dj

RUBINA KOTAK AND PETER MEIKLE
Astrophysics Group, Imperial College London, Blackett Laboratory, Prince Consort Road, London SW7 2AZ, UK; rubina@ic.ac.uk
SCHUYLER D. VAN DYK
Spitzer Science Center, California Institute of Technology, MS 220-6, Pasadena, CA 91125
PETER A. HÖFLICH
McDonald Observatory, University of Texas at Austin, 1 University Station, C1402, Austin, TX 78712-0259
AND
SEPPO MATTILA
Stockholm Observatory, Department of Astronomy, AlbaNova, 106 91 Stockholm, Sweden
Received 2005 May 5; accepted 2005 June 15; published 2005 July 14

ABSTRACT

We present mid-infrared observations with the *Spitzer Space Telescope* of the nearby Type II-P supernova SN 2004dj at epochs of 89–129 days. We have obtained the first mid-IR spectra of any supernova apart from SN 1987A. A prominent [Ni II] 6.64 μm line is observed, from which we deduce that the mass of stable nickel must be at least $2.2 \times 10^{-4}\ M_{\odot}$. We also observe the red wing of the CO fundamental band. We relate our findings to possible progenitors and favor an evolved star, most likely a red supergiant, with a probable initial mass between ~10 and 15 $M_{\odot}$.

Subject headings: supernovae: general — supernovae: individual (SN 2004dj)

Online material: color figures

1. INTRODUCTION

Core-collapse supernovae (SNe) are the endpoints of most stars more massive than ~8 $M_{\odot}$. As such, they provide a key test of stellar evolution. Furthermore, they play a major role in driving the chemical and dynamical evolution of galaxies and have also been proposed to be major contributors to dust at epochs when the universe was still young ($z \gtrsim 6$; e.g., Todini & Ferrara 2001).

SN explosions provide unique natural laboratories for studying, in real time, the physics of a variety of combustion, hydrodynamic, nuclear, and atomic processes. While SNe constitute important astronomical sources over all wavelength ranges, the combination of strong absorption by the Earth's atmosphere and the high background at mid-IR wavelengths has meant that this region has thus far remained inaccessible for the study of SNe, apart from the exceptionally nearby SN 1987A (e.g., Roche et al. 1993; Wooden et al. 1993).

Nevertheless, the mid-IR region holds the potential of providing unique insights into the nature of SN explosions and the role played by dust in these events. Although abundance measurements have long been carried out using UV/optical spectra, the large number of lines coupled with strong Doppler broadening leads to line blending, resulting in ambiguities in species identification and errors in flux measurement. In contrast, the fewer line transitions and much-reduced sensitivity to extinction in the mid-IR allow firm line identifications and accurate measurements of intrinsic line strength. Abundance measurements using fine-structure lines are particularly robust as these are largely insensitive to temperature. Furthermore, warm dust that may condense in the ejecta emits most strongly in the mid-IR. Moreover, by monitoring the mid-IR spectral energy distribution and evolution, we may discriminate between preexisting circumstellar dust and newly condensing dust in the ejecta.

The advent of the *Spitzer Space Telescope* (Werner et al. 2004), with its vastly improved mid-IR sensitivity/spatial resolution combination, compared with previous instrumentation, has finally opened up the possibility of studying typical nearby SNe in the mid-IR. In this Letter, we report on the first mid-IR results for SN 2004dj, the nearest SN in over a decade.

SN 2004dj was discovered in the nearby nearly face-on spiral galaxy NGC 2403 on 2004 July 31 by K. Itagaki at a visual magnitude of +11.2 (Nakano et al. 2004). It appears within a star cluster (Sandage 96; Sandage 1984; Maíz-Apellániz et al. 2004; Wang et al. 2005). A spectrum obtained on 2004 August 3 by Patat et al. (2004) revealed SN 2004dj to be a Type II-P (plateau) SN at an epoch of ~3 weeks postexplosion. In what follows, we assume an explosion date of 2004 July 10. Korcáková et al. (2005) present an *R*-band light curve that shows that the plateau phase had ended by about +100 days postexplosion. NGC 2403 lies within the M81 group at a distance of 3.13 Mpc (Freedman et al. 2001). About a month postexplosion, SN 2004dj was also detected at radio and X-ray wavelengths (Stockdale et al. 2004; Pooley & Lewin 2004).

2. OBSERVATIONS

SN 2004dj was observed with *Spitzer* as part of Director's Discretionary Time program 226. Here we report on the first two of four epochs with all three instruments (the Infrared Array Camera, Multiband Imaging Photometer for *Spitzer*, and Infrared Spectrograph; IRAC, MIPS, and IRS, respectively) at epochs of +89 to +139 days. Two further epochs of IRAC and MIPS images were serendipitously obtained from the *Spitzer* Investigation of Nearby Galaxies (SINGS) Legacy project (*Spitzer* PID 159; Kennicutt et al. 2003) in 2004 October.

2.1. *Photometry*

From the IRAC images it is clear that we have detected a source coincident with the position of SN 2004dj (Fig. 1). That this source is dominated by emission from the SN is evident from its fading with time (Table 1). Aperture photometry was carried out on the IRAC and MIPS (24 μm) post-BCD (basic calibrated data) image mosaics using GAIA. We

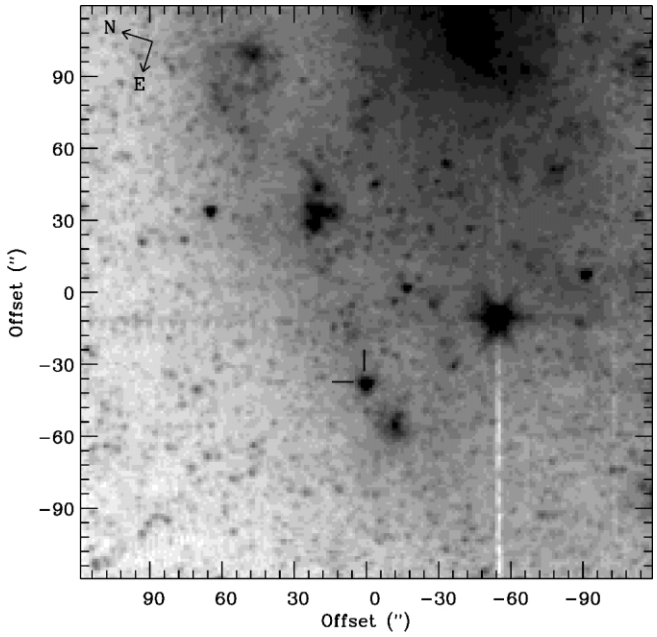

FIG. 1.—Subsection of a 3.6 μm *Spitzer* IRAC image taken at +89 days showing the immediate field around SN 2004dj. Short dashes mark the position of the SN ($\alpha = 7^h37^m17^s.2$, $\delta = +65°35'57''.8$ [J2000.0]), which lies 10″ north and 160″ east of the galaxy nucleus.

repeated the procedure for two IRAC epochs (+89 and +114 days) using the APEX software applied to the BCD frames and found generally consistent results. The results of our measurements are given in Table 1. The SN was not detected in the 70 and 160 μm MIPS channels, probably due to a combination of high host galaxy background and poorer spatial resolution in these channels.

Sugerman et al. (2005) have reported the rapid (5 day) decline of SN 2004dj at mid-infrared wavelengths. We point out that between +89 and 114 days the plateau phase was ending (Korcáková et al. 2005), which accounts for the rapid decline in the 3.6 and 8.0 μm channels during this time. The slower decline at the other two wavelengths is probably due to the emerging CO fundamental band emission (see § 3.1). There is also apparent evidence of a slower decline at 24 μm, but this is only significant at the 80% level. We therefore do not discuss it further.

2.2. *Spectroscopy*

Spectra were obtained on 2004 October 24 (+106 days) and 2004 November 16 (+129 days) using the Short-Low (SL; 5.2–14.5 μm, $R = 64$–128) and Long-Low (LL; 14–38 μm, $R = 64$–128) modules of the IRS. The observations were performed in staring mode. Total time on source for both epochs is 609.5 s in SL and 629.1 s in LL. Module slits were positioned relative to a reference star using a moderate-accuracy peak-up with the blue (16 μm) channel.

The SL data were preprocessed using version S11.0.2 of the *Spitzer* data processing pipeline. Subsequent reduction of these post-BCD data was carried out within the FIGARO 4 environment. We removed the background emission by differencing the two nod positions. For the first-order SL spectrum, the sky position (for both epochs) unfortunately landed on a cluster of bright sources, rendering it unusable. We therefore extracted the spectrum from the single uncontaminated nod position. We used the "tune" tables for the wavelength calibration. Flux calibration was carried out in two steps: each order was calibrated separately using the FLUXCON keywords provided. We then merged the spectra, manually clipping the ends of each order where the noise increases significantly. The spectra were scaled to match our day +114 IRAC channel 3, 4 photometry. The IRS epochs are, respectively, 8 days before and 15 days after this IRAC epoch, but no other postplateau IRAC points were available. However, the very slow mid-IR evolution of SN 1987A around these epochs suggests that the fluxing error introduced by the epoch differences is probably small. We applied scaling factors of 0.84 and 0.8 to the 106 and 129 day spectra, respectively. The uncertainty in these factors is ~15%, which probably dominates the overall fluxing error. We repeated the above reduction sequence for the +106 day spectrum, but this time starting from the BCD data, and found excellent agreement with the post-BCD results. The spectra are shown in Figure 2. The SN was not detected in the LL modules.

We supplemented the IRS data with 0.9–2.4 μm spectroscopy carried out on 2004 November 24 (+137 days) using the LIRIS instrument mounted at the Cassegrain focus of the William

TABLE 1
PHOTOMETRY OF SN 2004dj

			FLUX (mJy)				
			IRAC				MIPS
DATE	EPOCH (days)	t_{exp} (s)	3.6 μm	4.5 μm	5.8 μm	8.0 μm	24 μm
2004 Oct 7	+89	150	9.99 ± 0.03	7.60 ± 0.03	6.53 ± 0.05	4.09 ± 0.04	...
2004 Oct 10[a]	+92	240	10.82 ± 0.03	8.64 ± 0.03	6.15 ± 0.05	3.93 ± 0.04	...
2004 Oct 12[a]	+94	240	7.41 ± 0.03	8.43 ± 0.03	5.72 ± 0.05	3.39 ± 0.04	...
	+94	41.9	...	...	...	...	1.1 ± 0.3
2004 Oct 14	+96	165.7	...	...	...	...	1.2 ± 0.2
2004 Oct 16[a]	+98	41.9	...	...	...	...	1.0 ± 0.3
2004 Nov 1	+114	150	4.56 ± 0.02	6.67 ± 0.02	4.48 ± 0.04	2.48 ± 0.04	...
2004 Nov 6	+119	165.7	...	...	...	...	1.1 ± 0.2

NOTES.—The epochs are for an assumed explosion date of 2004 July 10 (Patat et al. 2004). The quantity t_{exp} is the on-source integration time. Photometry was carried out using a 3.″6 radius aperture for all four IRAC bands. Aperture corrections of 1.12, 1.12, 1.14, and 1.23 were applied to channels 1–4, respectively (see Table 5.7 of the IRAC data handbook). For the 24 μm MIPS data, we used a 5.″6 radius aperture (aperture correction = 1.72; MIPS data handbook, Fig. 3.2). Using a 6.″0 radius aperture for the MIPS 70 μm channel, we estimate a rough upper limit of 10 mJy. The t_{exp} at 70 and 160 μm is, respectively, 125.8 and 25.2 s for our setup, and 41.9 and 4.2 s for the SINGS setup. The errors shown are statistical errors only. Note that systematic errors in the calibration can be as large as 10%, although the relative errors are likely to be much smaller.

[a] Data for these dates are SINGS data.

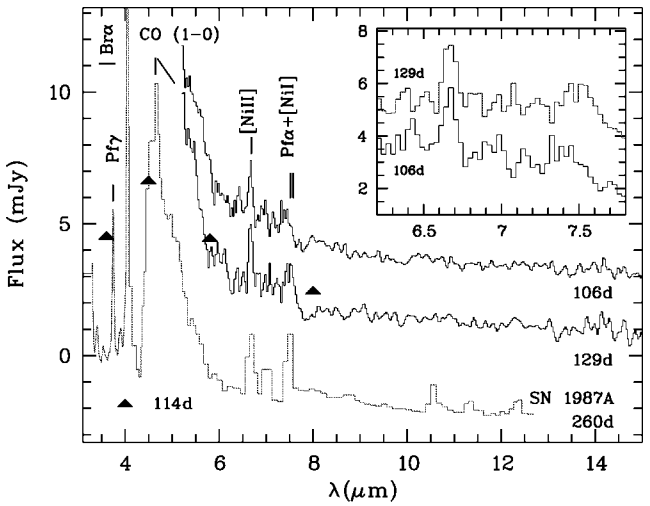

FIG. 2.—IRS spectra of SN 2004dj. The 106 day spectrum has been shifted by +2.5 mJy. The lowermost curve is the 260 day spectrum of SN 1987A (Meikle et al. 1989; Wooden et al. 1993); it has been arbitrarily scaled to highlight the striking similarity with SN 2004dj. The 114 day IRAC photometry is also shown. The inset zooms in on the 6.2–7.8 μm region of the SN 2004dj spectra (the 129 day spectrum has been shifted by +2.5 mJy) showing the profiles of the [Ni II] line and the emergence of the blend near 7.5 μm. [*See the electronic edition of the Journal for a color version of this figure.*]

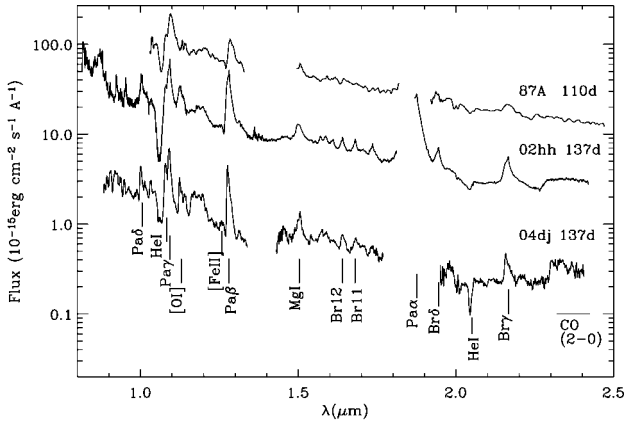

FIG. 3.—Comparison of the near-IR spectra of SN 2004dj with those of other, roughly coeval core-collapse SNe. All spectra have been corrected for redshift and reddening. The SN 2002hh spectrum has been taken from M. Pozzo et al. (2005, in preparation) and has been smoothed for display purposes. The SN 1987A spectrum has been taken from Meikle et al. (1989). We used $E(B-V)$ of 0.18 for SN 2004dj, 2.26 for SN 2002hh, and 0.19 for SN 1987A. The flux scale is appropriate for SN 2004dj only.

Herschel Telescope. These data were obtained using the low-resolution *ZJ* and *HK* grisms in the standard ABBA pattern with 10″ nods. The data were reduced in the usual fashion; the F6 dwarf BS 3028 was our chosen flux standard. Final fluxing was achieved by comparison with field stars in the *J*- and *H*-band acquisition images, calibrated using 2MASS data. The derived SN magnitudes are $J = +13.62 \pm 0.04$ and $H = +13.30 \pm 0.04$. We used these values to derive scaling factors ($ZJ = 1.14$ and $HK = 2.68$), which we applied to the near-IR spectrum shown in Figure 3. (The 2MASS preexplosion magnitudes of the underlying cluster are $J = +16.04 \pm 0.11$ and $H = +15.74 \pm 0.12$.)

3. ANALYSIS

3.1. *Carbon Monoxide*

The two IRS spectra show little difference in overall appearance. The bluemost region (see Fig. 2) is dominated by a rapidly rising slope that we identify with the red wing of the carbon monoxide fundamental (4.65 μm). This identification is reinforced by the clear detection of (1) the first overtone of CO at ~2.3 μm (Fig. 3) and (2) the growth with time of the excess flux in channels 2 and 3 compared with channels 1 and 4 (see Table 1).

Molecule formation provides a sensitive diagnostic of the conditions and degree of mixing in the SN ejecta. Cooling by CO sets the temperature structure, allowing the temperature to drop to $\lesssim$1600 K within a few photospheric radii. As it is optically thick, the CO fundamental band forms at several times the photospheric radius, while the first overtone forms close to the photosphere (defined to be where the Thomson scattering optical depth = 1). Thus, the ratio of the fundamental to the first overtone provides a powerful means for constraining both temperature and density. We use our near-simultaneous fundamental and first-overtone observations to investigate conditions in the SN 2004dj ejecta. Only a summary of first results is given here, as a more detailed analysis will be presented elsewhere.

We selected the explosion model from Chieffi et al. (2003) that best matched the plateau duration of SN 2004dj and adjusted the ^{56}Ni mass to match the radioactive tail. The parameters of this model were $M = 15\ M_\odot$, explosion energy = 10^{51} ergs, and $M(^{56}\mathrm{Ni}) = 0.03\ M_\odot$. Detailed radiative transport calculations were performed by solving the time-dependent rate equations for the formation of CO and SiO molecules, following Liu et al. (1992). We recalculated the temperature structure for the optically thin layers under the assumption of radiative equilibrium and evolved the model up to day 130, when the photosphere had receded well into the He-enriched layers, the structure of which depends on the details of several processes, e.g., mixing. We investigated the sensitivity to various parameters of CO formation by computing an exploratory grid of 36 models with the photospheric temperature, photospheric expansion velocity, and density profiles above the recombination zone in the range $3000\ \mathrm{K} \le T_{\mathrm{eff}} \le 5500$ K, $2000\ \mathrm{km\ s^{-1}} \le v_{\mathrm{exp}} \le 4000\ \mathrm{km\ s^{-1}}$, $-3 \le n \le -9$. We find a best fit with $T_{\mathrm{eff}} = 5500$ K and $n = 7$ (Fig. 4), values which corroborate a 15 $M_\odot$ progenitor.

The slope of the spectral energy distribution in the near-IR requires an underlying continuum to adequately fit the data (see Fig. 4). If this is due to dust from the SN, then given the relative youth of SN 2004dj, it is likely to be due to preexisting circumstellar dust, rather than newly condensing dust. A more likely source of this continuum is the underlying cluster. Using Starburst99 models, Maíz-Apellániz et al. (2004) infer that the cluster contains ≈12 red supergiants, which is broadly consistent with the near-IR flux from our data, as well as the preexplosion *J* and *H* magnitudes.

3.2. *Stable Nickel*

The other conspicuous feature in the SN 2004dj mid-IR spectra is a prominent emission feature at 6.67 μm, which we identify as the [Ni II] 6.634 μm fine-structure line. This is produced by the $a^2D_{3/2}$–$a^2D_{5/2}$ transition to the ground state. That this line is already visible at the start of the radioactive tail constrains the degree of mixing of the ejecta. The line is unresolved, indicating an expansion velocity of $\lesssim$3500 km s^{-1}. Its intensity at 106 days is $(1.1 \pm 0.1) \times 10^{-14}$ ergs s^{-1} cm^{-2}, rising to $(1.5 \pm 0.15) \times 10^{-14}$ ergs s^{-1} cm^{-2} on day 129. We used this line to estimate the mass of Ni$^+$. The critical density for the

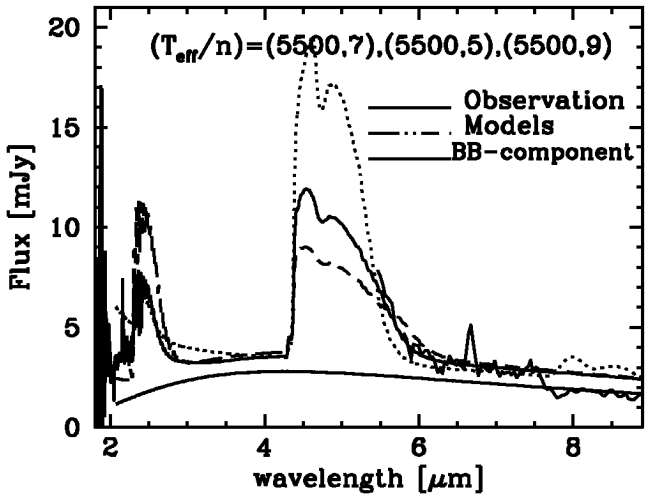

FIG. 4.—Comparison between observed and model profiles for the vibrational bands of CO on day 130. The models are identified by the ($T_{\rm eff}$, n)-tuples. To fit the observations, we have added a 1200 K blackbody component. Both n and $T_{\rm eff}$ have been varied to demonstrate the sensitivity of the emitted profiles to the physical conditions. Best agreement is obtained with $T_{\rm eff}$ = 5500 K and n = 7 (*dark gray solid curve*), which are close to those of the explosion model (see text). [*See the electronic edition of the Journal for a color version of this figure.*]

6.63 μm transition is 1.3×10^7 cm^{-3} (e.g., Wooden et al. 1993). At an epoch of ~100 days it is likely that the electron density was above this value. For example, Clocchiatti et al. (1996) estimate an electron density of 2.5×10^9 cm^{-3} within 2500 km s^{-1} for the Type II SN 1992H at 100 days. On this basis, we deem a simple LTE treatment to be valid. *A*-values were taken from Quinet & Le Dourneuf (1996) and partition function values from Halenka et al. (2001). The Ni$^+$ mass was estimated for 3000 and 6000 K. As expected, the result was rather insensitive to temperature. At 106 days and T = 3000 K we obtain $M(\mathrm{Ni}^+) = 1.7 \times 10^{-4}\ M_\odot$. Similar values were obtained with T = 6000 K. At 129 days we obtain $M(\mathrm{Ni}^+) = 2.2 \times 10^{-4}\ M_\odot$, again with similar values for both temperatures. Sobolev optical depths at the two epochs were ~0.2 and 0.4, respectively.

Given the clear presence of the [Ni II] 6.634 μm line, we examined the spectra for the [Ni I] 7.50 μm line, which is produced by the a^3F_3–a^3F_4 transition to ground. While there is little sign of this line at 106 days, by 129 days there is a feature whose red wing corresponds exactly to the expected location of the 7.50 μm line. We therefore suggest that the 7.50 μm line is present, but blended with another line to the blue. The most likely candidate is Pfα (7.46 μm). There may also be contributions to the observed feature from Huβ (7.50 μm) and H_{7-11} (7.51 μm). Consequently, direct measurement of the [Ni I] 7.50 μm line intensity is impractical. In a future paper, estimates will be made of the flux contribution from the H I lines in order to determine the intensity of the [Ni I] line.

At 129 days, virtually all the Ni must be made up of stable isotopes, dominated by ^{58}Ni. The derived mass can be regarded as a firm lower limit for the total stable Ni mass. As already indicated, it is likely that flux from Ni^0 is also present. Moreover, the [Ni II] line is close to being optically thick. The presence of a significant continuum suggests that yet more Ni lies below the photosphere.

3.3. *Constraints on the Progenitor Mass*

Following Hamuy (2003), we use the *V*-band luminosity of the exponential tail of the light curve[1] after 100 days to estimate the mass of ^{56}Ni. We find a mean mass of ~0.022 $M_\odot$, which suggests a progenitor mass of $\gtrsim$10 $M_\odot$ (Woosley & Timmes 1996) and is consistent with the value used in § 3.1.

Thielemann et al. (1996) predict stable Ni masses for core-collapse SNe having progenitor masses of 13–25 $M_\odot$. Up to 20 $M_\odot$, they predict masses of 0.007–0.013 $M_\odot$, but a much lower value of 0.002 $M_\odot$ for a 25 $M_\odot$ star. At this early epoch, our lower limit does not yet constrain this mass range. However, as the SN expands, we will be able to obtain a more definitive Ni mass estimate.

By fitting a variety of cluster spectral energy distributions, Maíz-Apellániz et al. (2004) have inferred that Sandage 96 is a 13.6 Myr cluster with a turnoff mass of 15 $M_\odot$ (but see Wang et al. 2005). Although they favor a red supergiant progenitor for SN 2004dj, they could not completely rule out a blue supergiant progenitor. Our CO analysis (§ 3.1) supports a red supergiant progenitor. This is indirectly supported by the lack of polycyclic aromatic hydrocarbon features (at 6.2, 7.7, 8.6, and 11.3 μm), which trace the far-UV stellar flux and, therefore, the young, hot stellar population (Peeters et al. 2004).

This work is based on observations made with the *Spitzer Space Telescope*, which is operated by the Jet Propulsion Laboratory, California Institute of Technology, under NASA contract 1407. Support for this work was provided by NASA through an award issued by JPL/Caltech. R. K. acknowledges support from the EC program "The Physics of Type Ia SNe" (HPRN-CT-2002-00303). We thank C. Gerardy for useful discussions, and M. Pozzo for providing the SN 2002hh spectrum (Fig. 3).

[1] Reported at http://www.astrosurf.com/snweb2/2004/04dj/04djCurv.htm.

REFERENCES

Chieffi, A., et al. 2003, MNRAS, 345, 111
Clocchiatti, A., et al. 1996, AJ, 111, 1286
Freedman, W. L., et al. 2001, ApJ, 553, 47
Halenka, J., Madej, J., Langer, K., & Mamok, A. 2001, Acta Astron., 51, 347
Hamuy, M. 2003, ApJ, 582, 905
Kennicutt, R. C., Jr., et al. 2003, PASP, 115, 928
Korcáková, D., et al. 2005, Inf. Bull. Variable Stars, 5605, 1
Liu, W., Dalgarno, A., & Lepp, S. 1992, ApJ, 396, 679
Maíz-Apellániz, J., et al. 2004, ApJ, 615, L113
Meikle, W. P. S., et al. 1989, MNRAS, 238, 193
Nakano, S., et al. 2004, IAU Circ. 8377
Patat, F., et al. 2004, IAU Circ. 8378
Peeters, E., Spoon, H. W. W., & Tielens, A. G. G. M. 2004, ApJ, 613, 986
Pooley, D., & Lewin, W. H. G. 2004, IAU Circ. 8390
Quinet, P., & Le Dourneuf, M. 1996, A&AS, 119, 99
Roche, P. F., Aitken, D. K., & Smith, C. H. 1993, MNRAS, 261, 522
Sandage, A. 1984, AJ, 89, 630
Stockdale, C. J., et al. 2004, IAU Circ. 8379
Sugerman, B., et al. 2005, IAU Circ. 8489
Thielemann, F.-K., Nomoto, K., & Hashimoto, M.-A. 1996, ApJ, 460, 408
Todini, P., & Ferrara, A. 2001, MNRAS, 325, 726
Wang, X., et al. 2005, ApJ, 626, L89
Werner, M., et al. 2004, ApJS, 154, 1
Wooden, D. H., et al. 1993, ApJS, 88, 477
Woosley, S. E., & Timmes, F. X. 1996, Nucl. Phys. A., 606, 137